UC Irvine
UC Irvine Previously Published Works

Title

Guanidine alkaloid analogs as inhibitors of HIV-1 Nef interactions with p53, actin, and p56lck

Permalink

https://escholarship.org/uc/item/6r9405g7

Journal

Proceedings of the National Academy of Sciences of the United States of America, 101(39)

ISSN

0027-8424

Authors

Olszewski, Allison

Sato, Ken

Aron, Zachary D

et al.

Publication Date

2004-09-28

DOI

10.1073/pnas.0406040101

Supplemental Material

https://escholarship.org/uc/item/6r9405g7#supplemental

Copyright Information

Peer reviewed

Guanidine alkaloid analogs as inhibitors of HIV-1 Nef interactions with p53, actin, and p56^{lck}

Allison Olszewski*, Ken Sato*, Zachary D. Aron*, Frederick Cohen*, Aleishia Harris†, Brenda R. McDougall†, W. Edward Robinson, Jr.†, Larry E. Overman*, and Gregory A. Weiss*‡§

Departments of *Chemistry, ‡Molecular Biology and Biochemistry, and †Pathology, University of California, Irvine, CA 92697-2025

With current anti-HIV treatments targeting only 4 of the 15 HIV proteins, many potential viral vulnerabilities remain unexploited. We report small-molecule inhibitors of the HIV-1 protein Nef. In addition to expanding the anti-HIV arsenal, small-molecule inhibitors against untargeted HIV proteins could be used to dissect key events in the HIV lifecycle. Numerous incompletely characterized interactions between Nef and cellular ligands, for example, present a challenge to understanding molecular events during HIV progression to AIDS. Assays with phage-displayed Nef from HIV$_{NL4-3}$ were used to identify a series of guanidine alkaloid-based inhibitors of Nef interactions with p53, actin, and p56^{lck}. The guanidines, synthetic analogs of batzellidine and crambescidin natural products, inhibit the Nef–ligand interactions with IC$_{50}$ values in the low micromolar range. In addition, sensitive *in vivo* assays for Nef inhibition are reported. Although compounds that are effective *in vitro* proved to be too cytotoxic for cellular assays, the reported Nef inhibitors provide proof-of-concept for disrupting a new HIV target and offer useful leads for drug development.

To counter the HIV pandemic, inhibitors targeting HIV protease, reverse transcriptase, and virus-cell fusion are currently available; integrase inhibitors are in clinical trials (1); and viral entry (2) and maturation inhibitors (3) are under development. However, current treatments do not target all HIV proteins, and expanding the anti-HIV repertoire may improve treatment options. For example, strains of HIV missing the gene encoding Nef can fail to progress to AIDS (4–6). Nef-deleted strains of HIV provide a genetic proof-of-concept for the potential efficacy of Nef inhibitors. Nef inhibition by the guanidine alkaloid congeners reported here could provide lead compounds for pharmaceutical development and tools for understanding the enigmatic roles of Nef in the HIV lifecycle.

The HIV-1 Nef protein is ≈200 aa in length, with the exact length varying by HIV isolate. The Nef C terminus and myristolyated N terminus are relatively flexible (7, 8). Although many cellular binding partners to Nef have been identified (9, 10), how Nef contributes to the viral lifecycle is not well understood; however, Nef expression is essential for HIV propagation and maintenance of viral loads (11, 12). Variations in Nef sequences isolated from HIV-infected individuals can also correlate with the rate of HIV progression (13). Nef interactions with CD4 (14–16) and major histocompatibility complex molecules (17, 18) are particularly important and can lead to down-regulation of key immune-system receptors.

Nef contributes to CD4 down-regulation by means of multiple interactions with cellular ligands. These interactions internalize CD4 and direct it to cellular-degradation pathways (19–21). For example, CD4 is usually protected from degradation by interaction with cellular p56^{lck} (19). Nef binding to p56^{lck} disrupts the CD4–p56^{lck} complex, exposing a CD4 dileucine motif and directing the protein to endocytic pathways (22, 23). Nef can tether the cytoplasmic tail of CD4 to adaptor-protein complexes on the surface of clathrin-coated pits, also leading to CD4 endocytosis (16). Moreover, Nef can link CD4 to the endosomal β-COP protein (16, 24), directing CD4 to the lysosome for degradation. Loss of CD4 has been correlated directly with increased HIV replication in T lymphocytes (15).

The N terminus of Nef (residues 1 to ≈57) is essential to interactions with p56^{lck}, p53, actin (25–28), and perhaps other cellular proteins. Nef binding to p53 can block p53-mediated apoptosis (26). The Nef interaction with actin could influence subcellular localizations of Nef (27, 28). Here, we demonstrate by ELISA that the N terminus of Nef from the NL4-3 infectious molecular clone of HIV is essential for Nef binding to p53, actin, and p56^{lck}. Because the Nef N terminus binds multiple targets, an inhibitor directed against this region of the protein could potentially block multiple Nef–ligand interactions during viral replication.

Guanidine alkaloids of the batzelladine family, which were isolated from the sponge *Crambe crambe*, can inhibit gp120–CD4 binding and induce CD4–p56^{lck} dissociation (29–31). Crambescidin guanidine alkaloids from the same sponge have also been shown to inhibit HIV-1 cell fusion (32, 33). The capability of guanidine-based natural products for disrupting these protein–protein interactions suggested that analogs of batzelladine and crambescidin alkaloids might inhibit other protein–protein interactions. In this article, selected batzelladine and crambescidin analogs are shown to disrupt Nef–p53, Nef–actin, and Nef–p56^{lck} interactions.

Materials and Methods

Nef-Phagemid Construction. The NL4-3 *nef* gene was cloned from HIV$_{NL4-3}$ (34) into a M13 phage display vector between the signal peptide and the *p8* gene with the *Nsi*I and *Afl*II restriction sites.

Compounds. Batzelladine and crambescidin analogs were synthesized as described (33, 35–38). Each compound was stored at −20°C at an average concentration of 10 mg/ml in DMSO.

ELISA of Phage-Displayed Nef. Cultures of *Escherichia coli* harboring individual phagemids were grown for 7 h at 37°C in 1 ml of 2YT medium (16 g of tryptone/10 g of yeast extract/5 g of NaCl per liter of water) and 50 μg/ml carbenicillin. M13-K07 helper phage (10^{10} phage per ml) was added, and cultures were transferred to 2YT medium (30 ml), supplemented with carbenicillin (50 μg/ml) and kanamycin (25 μg/ml), before incubation overnight at 37°C. Cells were removed by centrifugation (10 min at 8,000 × g), and the phage was precipitated from the supernatant by addition of 8 ml of 20% polyethylene glycol/2.5M NaCl. Phage were isolated by centrifugation (10 min at 8,000 × g and 2 min at 2,000 × g), resuspended in 1 ml of PBS (0.14 M NaCl/2.7 mM KCl/8 mM Na$_2$HPO$_4$/2 mM KH$_2$PO$_4$, pH 7.2, in 1 liter of water) and isolated by centrifugation (10 min at 8,000 × g). Phage concentration was determined by UV–Vis absorbance (OD$_{268}$ = 1, 8.31 × 10^{-9} M, 5 × 10^{12} phage per ml). Phages were

BIOCHEMISTRY

diluted to 5×10^{12} phage per ml in PBS. Specific wells of a 96-well Maxisorp immunoplate were coated with p53 (Santa Cruz Biotechnology), actin (Sigma), p56[lck] (Upstate Biotechnology, Charlottesville, VA), or anti-Nef antibody AE6 ascites (100 μl, 5 μg/ml in 50 mM carbonate buffer, pH 9.6) for 2 h at room temperature. The plate was then blocked for 30 min with ovalbumin (0.2%) in PBS and washed five times with PT buffer (0.05% Tween 20 in PBS). Separately, phage displaying HIV Nef were serially diluted with dilution buffer (0.2% ovalbumin/ 0.05% Tween 20/PBS). The phage solution was added directly to the corresponding wells of target-coated assay plates. The assay plates were shaken for 1 h at room temperature and washed five times with PT buffer. After washing, plates were incubated with anti-M13/horseradish peroxidase (HRP) conjugate (100 μl; 1:5,000 dilution, Amersham Biosciences) in dilution buffer for 30 min, and washed eight times with PT buffer and twice with PBS. Plates were developed with *o*-phenylenediamine dihydrochloride/H_2O_2 solution (100 μl; 1 mg/ml OPD/0.02% H_2O_2) in citric acid buffer (50 mM citric acid/50 mM Na_2HPO_4, pH 5.0). After 10 min, the absorbance was measured spectrophotometrically at 450 nm by using a 96-well microtiter-plate reader (μQuant, Bio-Tek, Burlington, VT). Phage-displayed Nef constructs were prepared from overnight cultures grown under identical conditions.

Small-Molecule Competition ELISA. Potential inhibitors were diluted 1:100 or 1:1,000 in deionized water. Dilution buffer (120 μl) was added to specific wells of a 96-well microtiter plate (Costar). For initial single-point screens of potential Nef inhibitors, compounds were added to specific wells for a final concentration of 5 μM. Phage displaying Nef (40 μl, to a final concentration of 2.8 nM) were added. The solutions of Nef and potential inhibitors were incubated for 1 h. The solutions (100 μl) from corresponding wells of the dilution plate were added to the blocked, ligand-bound assay plates, which were prepared as described above. The plate was developed as described. For dose–response assays of **14**, **17**, and **22**, inhibitors were prepared to a final concentration of 30 μM in water and diluted in dilution buffer. Phage-displayed Nef was added to each well, and the assay was performed as described for the single-point screens.

Direct Assay of Small-Molecule Binding. Crambescidin analog **47** was tested for binding to nonphage-displayed Nef (US Biologicals, Swampscott, MA), actin, or ovalbumin blocking agent. Maxisorp plates were coated with Nef (100 μl; 5 μg/ml in 50 mM carbonate buffer, pH 9.6) or actin (100 μl, 5 μg/ml) for 2 h at room temperature. The plate was blocked and washed as described for the phage-displayed ELISA. Crambescidin analog **47**, which was chosen for its availability, was diluted to a final concentration of 5.0 μM and incubated on the coated wells for 1 h (100 μl). The plate was washed seven times with PT buffer and three times with water, and 100 μl of 100 mM HCl was added to each well. We analyzed 80 μl of each well by reverse-phase HPLC–MS (model LCT, Waters). Crambescidin analog **47** was separated on a 2 mm $\times$ 15 cm C18 column by using a gradient from 98% solvent A (98% water/2% methanol/0.2% acetic acid) to 95% solvent B (methanol/0.2% acetic acid) over 20 min, followed by 7 min at solvent B before returning to solvent A over 3 min. With a flow rate of 0.2 ml/min, the retention time for crambescidin analog **47** was 23.2 min.

Assay for Compound Cytotoxicity and Anti-HIV Activity. We tested 18 compounds for cytotoxicity by the method described in ref. 39. Briefly, compounds were dissolved in ethanol, serially diluted, and incubated with MT-2 cells in triplicate. After cellular growth at 37°C for 72 h, cells were stained with Finter's neutral red dye, and the percentage of viable cells was quantified at 540 nm.

Generation of *nef*-Deleted HIV$_{NL4-3}$. A *Bam*HI–*Xho*I fragment encoding nucleotides 8,465–8,892 of HIV-1$_{NL4-3}$ (GenBank accession no. M19921), containing the first 105 nucleotides of *nef*, was subcloned into pGEX-4T (Pharmacia). QuikChange mutagenesis with *Pfu* DNA polymerase I (Stratagene) was used to introduce two stop codons (italicized) between nucleotides 8,847 and 8,852. The plus-strand primer (5′-GTAAGGGAAAGAATG*TGATGA*GCT-GAGCCAGCAGC-3′; nucleotides 8,832–8,866) and the minus-strand primer (5′-GCTGCTGGCTCAGC*TCATCA*CATTCTT-TCCCTTAC-3′; nucleotides 8,866–8,832) were used for this reaction. The mutations deleted a *Bsm*BI site, and the absence of this site was used to indicate successful mutagenesis. The DNA fragment containing the change was then ligated into HIV$_{NL4-3}$ to generate HIV$_{NL4-3\Delta nef}$.

Infectious-plasmid DNA was introduced into H9 cells by single-pulse electroporation at 200 mV for 50 msec. Cultures were grown and refed every other day in growth media (RPMI 1640 containing 25 mM Hepes/2 mM L-glutamine supplemented with 11.5% heat-inactivated FBS). Cells were monitored for infection by indirect immunofluorescence assay (40). When the cultures were 100% positive for HIV antigens, supernatant fluids were clarified of cells by low-speed centrifugation, followed by filtration through 0.45-μm pore-size cellulose acetate filters. Aliquots of HIV$_{NL4-3}$ and HIV$_{NL4-3\Delta nef}$ were frozen at -80°C until use.

Real-Time PCR. We inoculated 1×10^7 CD4$^+$ lymphoblastoid H9 cells in triplicate flasks with either HIV$_{NL4-3}$ or HIV$_{NL4-3\Delta nef}$ at $\approx 2.5 \times 10^6$ cpm of reverse-transcriptase activity, resulting in a final multiplicity of infection of <1.0. Cells were harvested and lysed for real-time PCR as described to measure minus-strand strong-stop DNA, completely synthesized HIV cDNA, or integrated HIV cDNA by using AA55/M667, M661/M667, and nested *alu* PCR primers, respectively (41, 42). Infections were monitored over the first 48 h, which includes the first round of replication (42).

HIV Spread. We inoculated $\approx 1.5 \times 10^7$ MT-2 CD4$^+$ lymphoblastoid cells with either HIV$_{NL4-3}$ or HIV$_{NL4-3\Delta nef}$ at $\approx 1.0 \times 10^6$ cpm of reverse-transcriptase activity, resulting in a final multiplicity of infection of <1.0. Cells were harvested at various times after infection and fixed by using 1:1 acetone/methanol. Cells were stained by using polyclonal human Ig containing antibodies to HIV and fluorescein-conjugated goat anti-human IgG. The percentage of HIV antigen-positive cells was determined by using an epifluorescent microscope (Nikon) as described (40, 42).

Results

Phage Display and Assay of HIV-1 Nef. After subcloning the *nef* gene into an appropriate phagemid, display of Nef on the surface of M13 phage was verified by phage ELISA by using three antibodies specific to Nef (data not shown). Phage-displayed full-length Nef (from HIV$_{NL4-3}$, residues 1–206) and core-domain Nef (residues 56–205) were examined by ELISA for binding to p53, actin, and p56[lck] (Fig. 1). Only full-length Nef bound to the three ligands, which confirms the requirement for the N terminus of Nef to mediate binding. By this assay, the three cellular ligands exhibited similar affinities for full-length Nef. Negative controls included binding of phage without Nef displayed (K07) to p53, actin, and p56[lck] and binding to the ovalbumin blocking agent by phage-displayed Nef; the negative controls exhibited greatly reduced binding (Fig. 1). Thus, the *in vitro* assays reported here examine interactions with full-length Nef. For a competition ELISA to identify potential small-molecule inhibitors of Nef, small molecules were added to a solution of phage-displayed full-length Nef and incubated for 1 h before binding to p53, actin, or p56[lck].
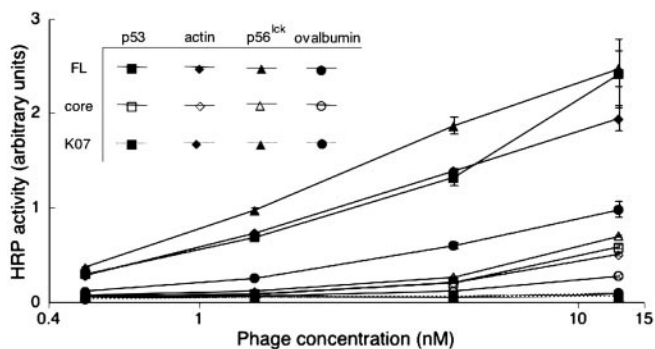
Fig. 1. Phage-displayed NL4-3 full-length (FL) or core domain (core) Nef binding to p53, actin, p56^{lck}, or ovalbumin. The negative control represents phage (K07) without displayed Nef. Error bars for all phage-displayed Nef binding data indicate SE for the average of three independent assays.

Screening Guanidine Alkaloids to Identify Nef Inhibitors. A library containing the natural products ptilomycalin A, batzelladine F, and 46 batzelladine- and crambescidin-based analogs (33, 37, 38) were initially screened by competition ELISA (Fig. 2 and Figs. 6 and 7, which are published as supporting information on the PNAS web site). The control compounds arginine, guanidine, tetramethylguanidine, and tetramethylguanidine trifluoroacetic acid salt were also assayed. At compound concentrations of 5 μM, nine guanidines from this library inhibited the three Nef–ligand interactions at levels of >80% (Table 1). Three compounds (**14**, **17**, and **22**) exhibited >94% inhibition of the three Nef–ligand interactions.

Inhibition of Nef Interactions with p53, Actin, and p56^{lck}. As shown by competition ELISA, addition of specific batzelladine and guanidine compounds at low micromolar concentrations decreased phage-displayed Nef affinity for p53, actin, and p56^{lck} to background levels. Interestingly, each compound exhibits similar
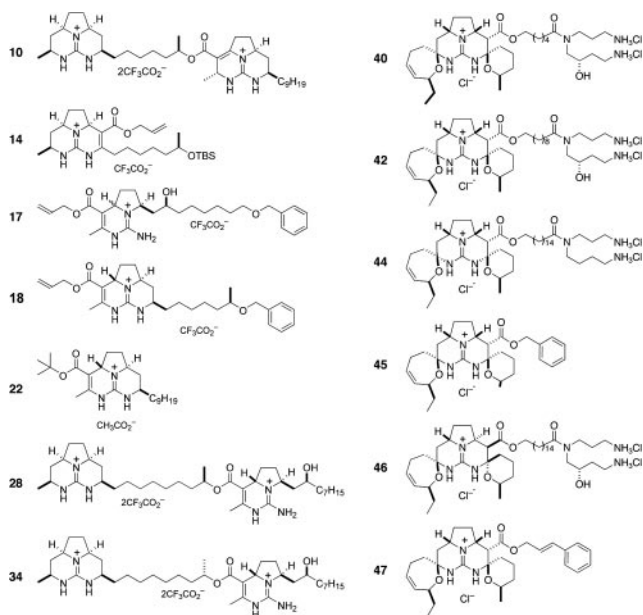

Fig. 2. Structures of batzelladine and crambescidin analogs. Depicted compounds inhibited at least one Nef–ligand interaction >80% in the initial competition ELISA. Compounds **14**, **17**, **22**, **28**, **42**, and **46** were identified by the initial screen as the most potent inhibitors of the three Nef–ligand interactions.

Table 1. Percentage of inhibition for the most effective Nef–ligand inhibitors at a compound concentration of 5 μM

Compound	% Inhibition
Nef–p53	
17	101.1 ± 2.3
22	96.8 ± 0.9
14	94.7 ± 1.0
42	93.9 ± 1.0
46	93.3 ± 0.6
28	87.2 ± 0.6
34	84.5 ± 1.8
45	82.9 ± 1.0
47	81.2 ± 0.4
44	81.0 ± 0.6
Nef–actin	
22	102.9 ± 0.4
17	102.4 ± 2.0
14	102.2 ± 0.4
42	89.5 ± 0.8
28	85.5 ± 1.1
18	85.4 ± 3.6
10	84.2 ± 0.5
46	83.9 ± 2.0
45	80.6 ± 1.0
47	78.1 ± 1.8
Nef–p56^{lck}	
17	101.0 ± 0.4
22	96.5 ± 0.4
14	95.8 ± 0.8
42	93.6 ± 1.4
46	89.3 ± 1.9
28	86.8 ± 0.6
18	82.7 ± 4.3
10	82.5 ± 1.0
40	80.6 ± 0.3
45	79.8 ± 1.7

Data are an average of three assays with the indicated SE.

relative efficacies for the different Nef–ligand interactions (Fig. 3). For example, the best inhibitors across each assay were **14**, **17**, and **22** (Table 1 and Fig. 2). Conversely, poor inhibitors failed to inhibit the three Nef–ligand interactions. In summary, compounds either inhibited all three or no Nef–ligand interactions. Additionally, overexpressed Nef, which was not displayed on the phage surface, was used to evaluate binding to crambescidin analog **47**. The compound bound to Nef but not to actin (Fig. 4).

The control compounds arginine, guanidine, tetramethylguanidine, and tetramethylguanidine trifluoroacetic acid salt can decrease Nef–ligand binding by up to 40%, but other guanidine alkaloid-based compounds are significantly more active. At low concentrations, DMSO, which was used here as a compound vehicle, slightly agonizes Nef interactions with p53, actin, and p56^{lck} (Fig. 3). The batzellidine and crambescidin inhibitors reported here do not indiscriminately inhibit other protein–protein interactions, as demonstrated by a competition assay with a control interaction between phage-displayed HIV-1 Vif and p55 Gag (data not shown and S. Arrantinis, A.O., and G.A.W., unpublished data).

***In Vivo* Assays for Anti-Nef Activity.** Sensitive assays were developed to quantitate the effects of Nef inhibitors on viral spread for cell culture-propagated HIV. First, stop-codon mutations were introduced into the *nef* gene in the HIV$_{NL4-3}$ background (HIV$_{NL4-3\Delta nef}$). Such mutations are expected to prevent Nef translation. A decrease in viral spread for HIV$_{NL4-3\Delta nef}$ was
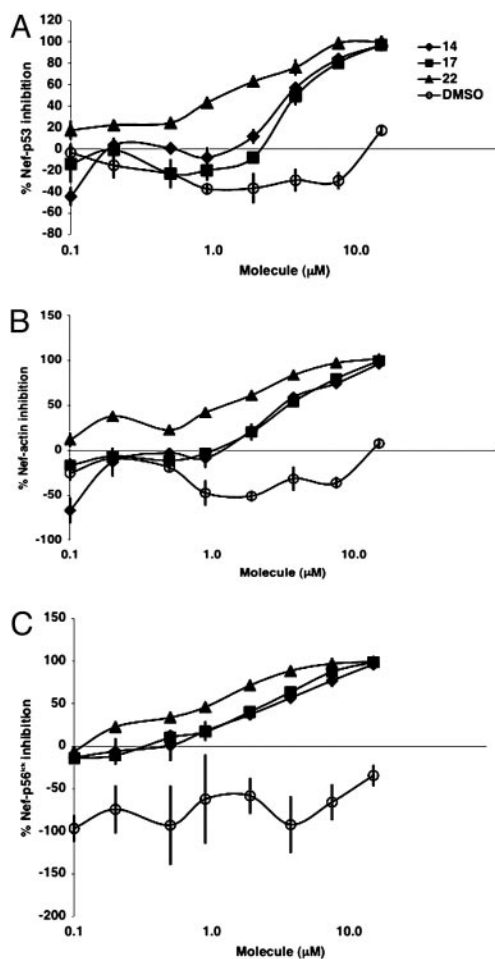
BIOCHEMISTRY

Fig. 3. Dose–response inhibition of phage-displayed Nef (2.8 nM) binding to p53 (*A*), actin (*B*), and p56^{lck} (*C*). Percentage of inhibition is relative to ligand binding by phage-displayed Nef without the addition of inhibitor or DMSO.
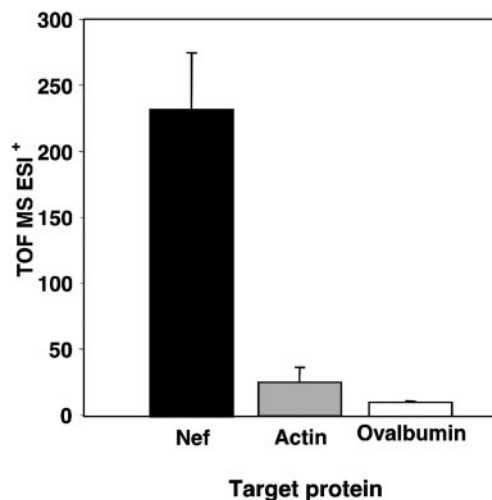

Fig. 4. Crambescidin analog 47 binding to Nef, actin, or ovalbumin negative control. Time-of-flight MS ESI$^+$ (TOF MS ESI$^+$) indicates the intensities of peaks at the expected retention time and molecular weight (520) of crambescidin analog 47. Error bars indicate the SE for the average of three independent assays.

observed (Fig. 5). These results were confirmed with analysis by real-time PCR. Measurement of minus-strand strong-stop DNA, the first product of reverse transcription, and completely synthesized HIV cDNA, the final product of reverse transcription, demonstrated that HIV$_{NL4-3\Delta nef}$ was defective for spread after an inefficient initial infection (Fig. 5 *A* and *B*). This experiment also resulted in little integrated HIV cDNA (Fig. 5*C*). Finally, when measuring HIV-antigen synthesis, HIV lacking Nef fails to spread with the same efficiency as virus containing an intact *nef* gene (Fig. 5*D*). Results were the same when using HIV with the *nef* gene deleted (data not shown). HIV$_{NL4-3\Delta nef}$ demonstrated similar replication defects in both H9 (Fig. 5 *A–C*) and MT-2 cells (Fig. 5*D*). These experiments demonstrate that compounds capable of disrupting Nef activity could have dramatic effects on HIV replication in cell culture. Such activities can be readily detected by either immunofluorescence or real-time PCR assays.

We chose 18 compounds, including **14**, **17**, and **22**, for assays to quantitate anti-HIV activity. However, at submicromolar concentrations, all compounds were cytotoxic to MT-2 cells (data not shown). Unfortunately, this cellular toxicity prevents experiments with the 18 compounds to assess anti-HIV effects in human cell cultures.

Discussion

***In Vitro* Screens for Nef Inhibition.** Phage display has been used to explore complex protein–protein interactions, such as mapping functional epitopes and uncovering binding partners (43, 44). The technique also offers a sensitive format for high-throughput screening of inhibitors to the phage-displayed protein. For example, enzyme inhibitors have been identified from phage-displayed peptide libraries, and the resultant peptides have been used for high-throughput, small-molecule screening (45). The *in vitro* Nef–ligand screens described here represent what is, to our knowledge, the first application of phage display applied to the identification of protein–protein inhibitors. The technique offers some potential advantages over conventional protein–protein interaction screens, which often require cumbersome additional steps, such as biotinylation or fluorescent labeling of one target protein. Advantages of the phage-display technique include sensitive, robust binding assays and rapid adaptability of the target protein. Altering the phage-displayed protein to target a different protein variant requires a simple one-step mutagenesis. Other ELISAs to examine Nef–ligand interactions (including to p53, actin, and p56^{lck}) have been reported (26, 27, 46).

To demonstrate the adaptability of phage display-based assays, we examined the importance of the N terminus of Nef to interactions with the cellular ligands p53, actin, and p56^{lck}. Binding to full-length and core HIV$_{NL4-3}$ Nef was compared. Anti-Nef antibodies and a similar ELISA format were used to verify the approximately equivalent display levels for the two constructs (data not shown). Essentially, no binding to the three ligands was observed for phage-displayed core Nef (Fig. 1). The requirement for the N terminus of Nef to mediate binding to p53, actin, and p56^{lck} confirms known binding preferences (25–27) and demonstrates the efficacy of the assay. The reported phage-displayed binding assay could also be adapted for Nef library selections and screens.

Small-Molecule Nef Inhibitors. Next, we sought to determine whether the *in vitro* Nef assays reported here could be used to identify small molecules capable of disrupting Nef binding activities. Batzellidine and crambescidin alkaloids quickly became the focus of our efforts because of the known abilities for some batzellidine and crambescidin derivatives to disrupt other protein–protein interactions, including CD4 binding to p56^{lck} (29, 30, 32). Competition-binding data demonstrate inhibition of three Nef–ligand interactions by batzellidine and
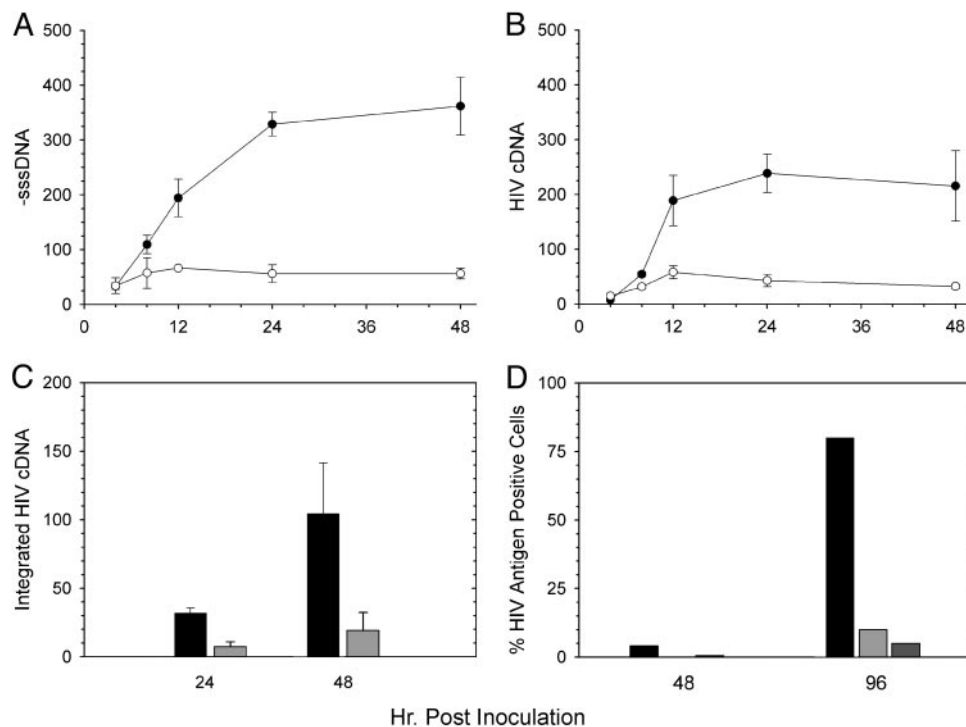
Fig. 5. Replication of HIV$_{NL4-3\Delta nef}$ in CD4$^+$ lymphoblastoid cell lines. The first round of replication for HIV$_{NL4-3\Delta nef}$ (○) in H9 cells was compared with HIV$_{NL4-3}$ containing an intact *nef* gene (●) by real-time PCR to measure minus-strand strong-stop DNA synthesis (*A*) and completely synthesized HIV cDNA (*B*). (*C*) Integrated HIV cDNA (provirus) was also quantified for both HIV$_{NL4-3\Delta nef}$ (light-gray bars) and HIV$_{NL4-3}$ (dark-gray bars). (*D*) Replication of two distinct clones of HIV$_{NL4-3\Delta nef}$ (light-gray and medium-gray bars) as measured by an immunofluorescence assay was also decreased compared with HIV$_{NL4-3}$ (black bars) in MT-2 cells. In *A–C*, data are the average from three infections; error bars are one SD. Values are in equivalent numbers of chronically HIV-infected H9 cells (41, 42). Cells were infected with equal amounts of each clone based on input reverse-transcriptase activity.

crambescidin analogs (Fig. 3). As described above, the three cellular ligands, p53, actin, and p56^{lck}, all bind to the N terminus of Nef. The ranking of best to worst inhibitor is essentially conserved across the three Nef–ligand assays (see Table 1 and Figs. 6 and 7). Additionally, overexpressed Nef, which is not displayed on the phage surface, binds crambescidin analog **47**. However, crambescidin analog **47** fails to bind actin or the ovalbumin negative control (Fig. 4). Together, the data conclusively demonstrate that the identified compounds inhibit Nef–ligand interactions primarily by binding to Nef and not the cellular ligand.

Guanidines **14**, **17**, and **22** were the most potent inhibitors of the three Nef–ligand interactions (Table 1 and Fig. 2). The crambescidin alkaloid ptilomycalin A (**44**) was a slightly weaker inhibitor, whereas batzelladine F (**26**) showed low activity. In general, members of the library that contained two guanidine subunits were poor inhibitors. The aliphatic side chains of the best inhibitors are highly flexible, which could permit these molecules to assume various binding conformations. The conserved bicyclic or tricyclic guanidine motif of the best inhibitors suggests that this functionality is essential for modulating Nef inhibition. These guanidine units could form bidentate hydrogen bonds to an appropriate Nef functionality, possibly a carboxylate side chain.

The Nef-inhibitory activity reported here provides another example of protein–protein inhibition by guanidine alkaloids. Various batzellidine and crambescidin alkaloids have been reported to inhibit gp120–CD4, CD4–p56^{lck}, and HIV-1 cell-fusion protein–protein interactions (29–33). With the planar guanidine functionality surrounded by hydrophobic rings, molecules of this class are ideally suited to disrupt the large, relatively flat surfaces common to protein–protein interactions.

Interest in this class of molecules has been partially motivated by the cytotoxic properties of the natural variants. Having identified a large number of active compounds, tissue culture-based assays were developed to examine the potential for inhibiting Nef *in vivo*.

***In Vivo* Assay of Nef Inhibitors.** Because Nef is an acronym for "*n*egative *e*ffector of HIV *f*unction," we were pleased to observe clearly distinguishable effects for growth of HIV constructs with a deleted or stop codon-terminated *nef* gene (Fig. 5). Cytotoxicity assays applied the methods reported in ref. 39. Unfortunately, high cytotoxicity for 18 guanidine alkaloids with *in vitro* Nef inhibitory activities precluded determination of *in vivo* anti-HIV activities.

In summary, we report small-molecule HIV-1 Nef inhibitors and analysis of HIV$_{NL4-3\Delta nef}$ by real-time PCR. Although the inhibitors proved to be too cytotoxic for anti-HIV assays, the assays and structure–activity relationship data reported here can guide development of Nef inhibitors. Such inhibitors could provide insight into the cellular consequence of Nef binding to p53, actin, and p56^{lck}. Other Nef–ligand interactions could require the Nef N terminus, and the reported compounds could also inhibit such interactions.

BIOCHEMISTRY

1. Gulick, R. M. (2003) *Clin. Microbiol. Infect.* **9,** 186–193.
2. Lin, P.-F., Blair, W., Wang, T., Spicer, T., Guo, Q., Zhou, N., Gong, Y.-F., Wang, H.-G. H., Rose, R., Yamanaka, G., *et al*. (2003) *Proc. Natl. Acad. Sci. USA* **100,** 11013–11018.
3. Li, F., Goila-Gaur, R., Salzwedel, K., Kilgore, N. R., Reddick, M., Matallana, C., Castillo, A., Zoumplis, D., Martin, D. E., Orenstein, J. M., *et al*. (2003) *Proc. Natl. Acad. Sci. USA* **100,** 13555–13560.
4. Salvi, R., Garbuglia, A. R., Di Caro, A., Pulciani, S., Montella, F. & Benedetto, A. (1998) *J. Virol.* **72,** 3646–3657.
5. Kirchhoff, F., Greenough, T. C., Brettler, D. B., Sullivan, J. L. & Desrosiers, R. C. (1995) *N. Engl. J. Med.* **332,** 228–232.
6. Deacon, N. J., Tsykin, A., Solomon, A., Smith, K., Ludford-Menting, M., Hooker, D. J., McPhee, D. A., Greenway, A. L., Ellett, A., Chatfield, C., *et al*. (1995) *Science* **270,** 988–991.
7. Geyer, M. & Peterlin, B. M. (2001) *FEBS Lett.* **496,** 91–95.
8. Geyer, M., Munte, C. E., Schorr, J., Kellner, R. & Kalbitzer, H. R. (1999) *J. Mol. Biol.* **289,** 123–138.
9. Arold, S. T. & Baur, A. S. (2001) *Trends Biochem. Sci.* **26,** 356–363.
10. Geyer, M., Fackler, O. T. & Peterlin, B. M. (2001) *EMBO Rep.* **2,** 580–585.
11. Kestler, H. W., III, Ringler, D. J., Mori, K., Panicali, D. L., Sehgal, P. K., Daniel, M. D. & Desrosiers, R. C. (1991) *Cell* **65,** 651–662.
12. Greenway, A. L., Holloway, G. & McPhee, D. A. (2000) *Adv. Pharmacol.* **48,** 299–343.
13. Kirchhoff, F., Easterbrook, P. J., Douglas, N., Troop, M., Greenough, T. C., Weber, J., Carl, S., Sullivan, J. L. & Daniels, R. S. (1999) *J. Virol.* **73,** 5497–5508.
14. Stoddart, C. A., Geleziunas, R., Ferrell, S., Linquist-Stepps, V., Moreno, M. E., Bare, C., Xu, W., Yonemoto, W., Bresnahan, P. A., McCune, J. M. & Greene, W. C. (2003) *J. Virol.* **77,** 2124–2133.
15. Lundquist, C. A., Tobiume, M., Zhou, J., Unutmaz, D. & Aiken, C. (2002) *J. Virol.* **76,** 4625–4633.
16. Piguet, V., Gu, F., Foti, M., Demaurex, N., Gruenberg, J., Carpentier, J.-L. & Trono, D. (1999) *Cell* **97,** 63–73.
17. Schindler, M., Würfl, S., Benaroch, P., Greenough, T. C., Daniels, R., Easterbrook, P., Brenner, M., Münch, J. & Kirchhoff, F. (2003) *J. Virol.* **77,** 10548–10556.
18. Cohen, G. B., Gandhi, R. T., Davis, D. M., Mandelboim, O., Chen, B. K., Strominger, J. L. & Baltimore, D. (1999) *Immunity* **10,** 661–671.
19. Kim, Y.-H., Chang, S. H., Kwon, J. H. & Rhee, S. S. (1999) *Virology* **257,** 208–219.
20. Bandres, J. C., Shaw, A. S. & Ratner, L. (1995) *Virology* **207,** 338–341.
21. Cheng, H., Hoxie, J. & Parks, W. P. (1999) *Virology* **264,** 5–15.
22. Aiken, C., Konner, J., Landau, N. R., Lenburg, M. E. & Trono, D. (1994) *Cell* **76,** 853–864.
23. Grzesiek, S., Stahl, S. J., Wingfield, P. T. & Bax, A. (1996) *Biochemistry* **35,** 10256–10261.
24. Benichou, S., Bomsel, M., Bodéus, M., Durand, H., Douté, M., Letourneur, F., Camonis, J. & Benarous, R. (1994) *J. Biol. Chem.* **269,** 30073–30076.
25. Baur, A. S., Sass, G., Laffert, B., Willbold, D., Cheng-Mayer, C. & Peterlin, B. M. (1997) *Immunity* **6,** 283–291.
26. Greenway, A. L., McPhee, D. A., Allen, K., Johnstone, R., Holloway, G., Mills, J., Azad, A., Sankovich, S. & Lambert, P. (2002) *J. Virol.* **76,** 2692–2702.
27. Fackler, O. T., Kienzle, N., Kremmer, E., Boese, A., Schramm, B., Klimkait, T., Kücherer, C. & Mueller-Lantzch, N. (1997) *Eur. J. Biochem.* **247,** 843–851.
28. Campbell, E. M., Nunez, R. & Hope, T. J. (2004) *J. Virol.* **78,** 5745–5755.
29. Patil, A. D., Kumar, N. V., Kokke, W. C., Bean, M. F., Freyer, A. J., De Brosse, C., Mai, S., Truneh, A., Faulkner, D. J., Carte, B., *et al*. (1995) *J. Org. Chem.* **60,** 1182–1188.
30. Patil, A. D., Freyer, A. J., Taylor, P. B., Carté, B., Zuber, G., Johnson, R. K. & Faulkner, D. J. (1997) *J. Org. Chem.* **62,** 1814–1819.
31. Patil, A. D., Freyer, A. J., Offen, P., Bean, M. F. & Johnson, R. K. (1997) *J. Nat. Prod.* **60,** 704–707.
32. Chang, L., Whittaker, N. F. & Bewley, C. A. (2003) *J. Nat. Prod.* **66,** 1490–1494.
33. Bewley, C. A., Ray, S., Cohen, F., Collins, S. K. & Overman, L. E. (July 8, 2004) *J. Nat. Prod.*, 10.1021/np049958o.
34. Adachi, A., Gendelman, H. E., Koenig, S., Folks, T., Willey, R., Rabson, A. & Martin, M. A. (1986) *J. Virol.* **59,** 284–291.
35. Cohen, F. & Overman, L. E. (2001) *J. Amer. Chem. Soc.* **123,** 10782–10783.
36. Cohen, F., Overman, L. E. & Ly Sakata, S. K. (1999) *Org. Lett.* **1,** 2169–2172.
37. Aron, Z. D., Pietraszkiewicz, H., Overman, L. E., Valeriote, F. & Cuevas, C. (2004) *Bioorg. Med. Chem. Lett.* **14,** 3445–3449.
38. Coffey, D. S., McDonald, A. I., Overman, L. E., Rabinowitz, M. H. & Renhowe, P. A. (2000) *J. Amer. Chem. Soc.* **122,** 4893–4903.
39. Montefiori, D. C., Robinson, W. E., Jr., Schuffman, S. S. & Mitchell, W. M. (1988) *J. Clin. Microbiol.* **26,** 231–235.
40. Robinson, W. E., Jr., Montefiori, D. C., Gillespie, D. H. & Mitchell, W. M. (1989) *J. Acquired Immune Defic. Syndr.* **2,** 33–42.
41. Victoria, J. G., Lee, D. J., McDougall, B. R. & Robinson, W. E., Jr. (2003) *AIDS Res. Hum. Retroviruses* **19,** 865–874.
42. Lee, D. J. & Robinson, W. E., Jr. (2004) *J. Virol.* **78,** 5835–5847.
43. Sidhu, S. S., Fairbrother, W. J. & Deshayes, K. (2003) *ChemBioChem* **4,** 14–25.
44. Diaz, J. E., Howard, B. E., Neubauer, M. S., Olszewski, A. & Weiss, G. A. (2003) *Curr. Issues Mol. Biol.* **5,** 129–146.
45. Hyde-DeRuyscher, R., Paige, L. A., Christensen, D. J., Hyde-DeRuyscher, N., Lim, A., Fredericks, Z. L., Kranz, J., Gallant, P., Zhang, J., Rocklage, S. M., *et al*. (2000) *Chem. Biol.* **7,** 17–25.
46. Greenway, A., Azad, A., Mills, J. & McPhee, D. A. (1996) *J. Virol.* **70,** 6701–6708.

1 2CF₃CO₂⁻
2 2CF₃CO₂⁻
3 2CF₃CO₂⁻
4 2CF₃CO₂⁻ NH₂
5 2CF₃CO₂⁻ NH₂
6 2CF₃CO₂⁻
7 2CF₃CO₂⁻ NH₂
8 2CF₃CO₂⁻ NH₂
9 CF₃CO₂⁻
10 2CF₃CO₂⁻
11 2CF₃CO₂⁻
12 2CF₃CO₂⁻
13 2CF₃CO₂⁻ NH₂
14 CF₃CO₂⁻ OTBS
15 BF₄⁻
16 CF₃CO₂⁻
17 NH₂ CF₃CO₂⁻
18 CF₃CO₂⁻

19 CH₃CO₂⁻ NH₂
20 CF₃CO₂⁻
21 Br⁻ Cl⁻
22 CH₃CO₂⁻
23 2CF₃CO₂⁻
24 2CF₃CO₂⁻
25 2CF₃CO₂⁻
26 2CF₃CO₂⁻
27 BF₄⁻
28 2CF₃CO₂⁻ NH₂
29 2CF₃CO₂⁻
30 BF₄⁻
31 2CF₃CO₂⁻
32 CF₃CO₂⁻ OTBS
33 NH₂⁺ NH₂ Cl⁻ OMe OMe
34 2CF₃CO₂⁻ NH₂
35 2CF₃CO₂⁻
36 2CF₃CO₂⁻

37 2CF₃CO₂⁻
38 2CF₃CO₂⁻
39 2CF₃CO₂⁻
40 Cl⁻ NH₃Cl NH₃Cl OH
41 Cl⁻
42 Cl⁻ NH₃Cl NH₃Cl OH
43 Cl⁻
44 Cl⁻ NH₃Cl NH₃Cl
45 Cl⁻
46 Cl⁻ NH₃Cl NH₃Cl OH
47
48